Dual-Independent Active Sites for Efficient Hydrogen Production

Yangyang Feng [a†]*, *Yongxin Guan* [b†]*, *Lei Wen* [b], *Yunxia Liu* [b]

[a]CAS Key Laboratory of Design and Assembly of Functional Nanostructures, and Fujian Provincial Key Laboratory of Nanomaterials, State Key Laboratory of Structural Chemistry, Fujian Institute of Research on the Structure of Matter, Chinese Academy of Sciences, Fuzhou 350002, Fujian, P. R. China.

[b]Key Laboratory of Material Processing and Mold Technology, School of Architectural Engineering, Chongqing Industry Polytechnic College, Chongqing 401120, China.

[†]These authors contributed equally to this work

***** Corresponding author

Materials and methods

Materials:

Cobalt nitrate ($Co(NO_3)_2$, Aldrich, 99.9%), Sodium molybdate (Na_2MO_4, Aldrich, 99.9%), Glucose (Alfa), Sodium Carbonate (Na_2CO_3, Aldrich, 99.9%), Ammonia Hydroxide ($NH_3 \cdot H_2O$, Aldrich, 28-30 wt%), Molybdenum carbide (Mo_2C, 99%) .

Sample preparation

Preparation of Mo_2C@C/Co@C:

The preparation of MoCo hydroxide precursor: 2.5 mmol Na_2MoO_4 and 2.5 mmol $Co(NO_3)_2$ were gradually put into 40 mL D.I. water with strong stirring. Then the solution was continued to stir for 15 min. After stirring, the mixture was poured into the 50 mL autoclave and transferred into an oven at 150 ^oC for 6 h. After reaction, the sample was precipitated at the bottle of the autoclave and then washed several times by

D.I. water and ethanol to remove the impurities. Finally, the precursor was dried in a vacuum oven for 12 h.

The polymerized glucose coating: the precursor (100 mg) and glucose (0.5 mM) were mixed in deionized water (40 mL). The solution after uniform mixing was transferred into autoclave for carbon coating (180 ^{o}C, 8 h). Then, cleaning and washing the as-obtained intermediate products by D.I. water and ethanol, and drying overnight at 60 ^{o}C.

The preparation of Mo_2C@C/Co@C: the polymerized glucose-coated sample was put into tube furnace under calcination in Ar to form Mo_2C@C/Co@C under 700 ^{o}C for 200 min.

Preparation of Co NPs: The 12.5 mL $NH_3 \cdot H_2O$ (28 wt%), 12.5 mL ethylene glycol, 5 mL 1 M Co $(NO_3)_2$ aqueous solution and 5 mL 1 M Na_2CO_3 aqueous solution were mixed together. After strong stirring for about 10 min, the mixture was transferred into the autoclave with a volume of 50 mL and calcinated at 170°C for 16 h in the oven. After washing and drying, the precursor was put into tube furnace under Ar/H_2 at 700 ^{o}C for 200 min.

Characterization

The morphology characterizations were investigated by scanning electron microscope (SEM, FEI, JSM-7800F) under the voltage of 5 kV, energy dispersive spectrometer analyzer (EDS), and transmission electron microscope (TEM, Tecnai, 300 kV). The phase and structure characterizations are tested by X-ray diffractometer (XRD, Bruker

ECO D8 power) under Cu Ka with the 2 theta of 10-90°, X-ray photo electron spectrometer (XPS, ESCALAB 250Xi, Thermo scientific, 225 W, 15 mA, 15 kV Al Kα), Raman microscope (Renishaw Invia, laser: 532 nm) and BET specific-surface-area pore-size analyzer (Quantachrome Autosorb-6B).

Electrochemical Measurements:

Electrochemical properties were conducted on CHI660 workstation by a three-electrode setup, which includes carbon rod, reference electrode and catalyst. The saturated calomel electrode (SCE) was used as a reference electrode in 1.0 M KOH with various hydrazine. Linear sweep voltammetry (LSV) was performed at the scan rates of 5 mV/s from -1.7 to -1.0 V and -1.2 to -0.8 V for HER and HzOR, respectively. The Tafel slope was obtained by fitting the linear portion of the Tafel plots to the Tafel equation of [$\eta = b \log(j)+a$]. The electrochemical active surface areas (ECSAs) were estimated in 1.0 M KOH by calculating the double-layer capacitances (C_{dl}) at the solid-liquid interface from cyclic voltammograms (CVs) method at the scan rates of 10-120 mV/s. ECSA in this work was calculated by electrochemical double layer capacitence (C_{dl}) values via the following equation:

$$ECSA = \frac{C_{dl}}{C_s}$$

C_s refers to the specific capacitance which is calculated through smooth planar surface. The specific capacitance on the smooth surface is accepted to be during 20 to 60 μF/cm^2. In this manuscript, we assumed 40 μF/cm^2.

In all measurements, the reference electrode was calibrated with respect to the reversible hydrogen electrode (RHE).

OHzS electrolyzer: OHzS test was conducted in 1 M KOH/0.2 M N_2H_4 with Mo_2C@C/Co@C as anode and cathode.

Zn-Hz battery with Mo_2C@C/Co@C cathode: The aqueous rechargeable Zn-Hz battery test was conducted in a double-electrolyte system separated by anion-exchange membrane. The cathodic compartment was filled with 1 M KOH with 0.2 M N_2H_4 and the anodic electrolyte was 1 M KOH and 0.02 M $Zn(CH_3COO)_2$. A Zn plate after mechanical polishing with sandpaper with an area of 2×5 cm^2 was applied as the anode and carbon paper (0.5×0.5 cm) with catalyst as cathode.

Theoretical calculations

Calculations in this work were performed using the CASTEP code by Vienna ab Initio Simulation package (VASP). The interaction between core and valence electrons is presented by standard PAW potentials. The correlation functional and electron-electron exchange were described via Perdew-Burke-Ernzerhorf generalized gradient approximation (PBE-GGA). The electron wave function was in plane-wave with the cutoff energy of 450 eV in all computations with the force threshold of 0.01 eV/ Å.

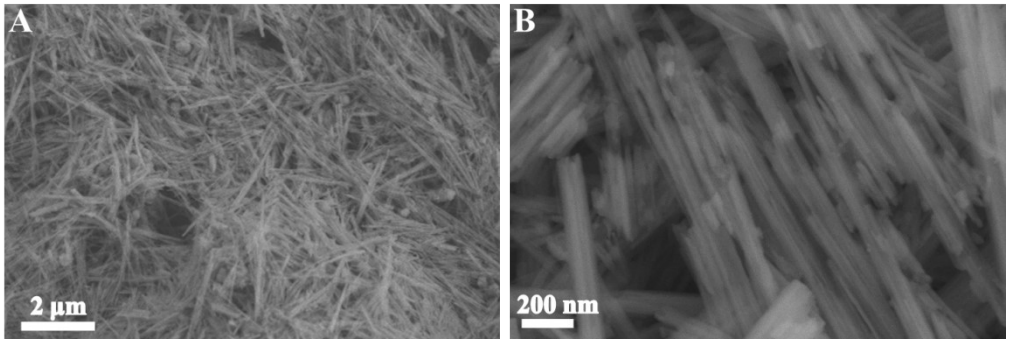

Figure S1. SEM images of rod-like MoCo hydroxide in different resolutions.

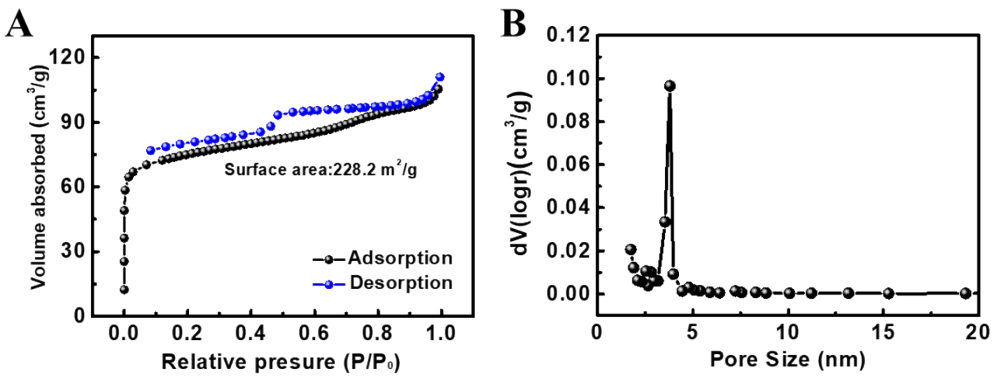

Figure S2. A) BET profile of Mo_2C@C/Co@C to reveal the specific surface area and B) pore size distribution derived from the desorption branch.

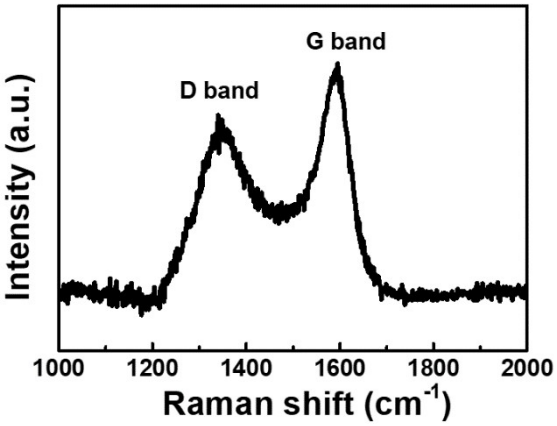

Figure S3. Raman spectrum of Mo_2C@C/Co@C.

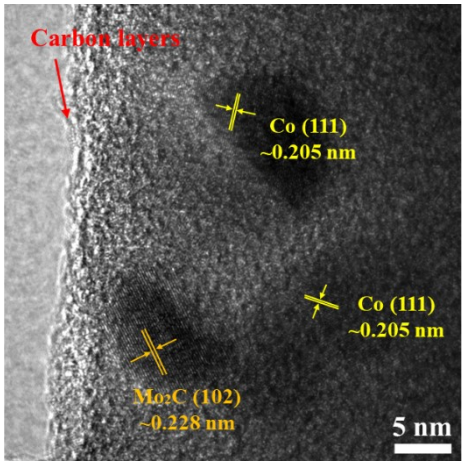

Figure S4. HRTEM image of Mo_2C@C/Co@C.

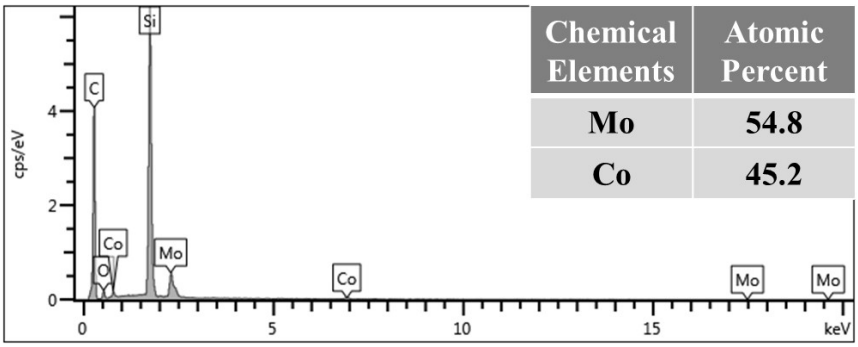

Chemical Elements	Atomic Percent
Mo	54.8
Co	45.2

Figure S5. The corresponding EDS of Mo_2C@C/Co@C.

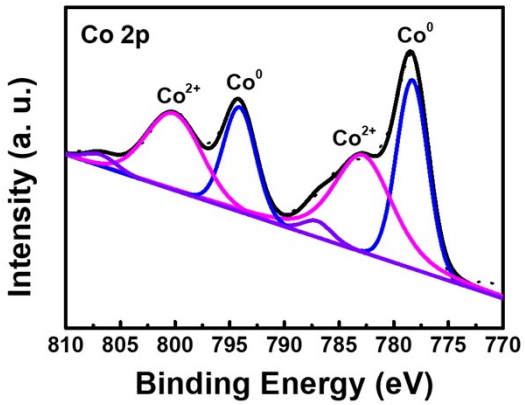

Figure S6. The XPS spectrum of Co 2p in Mo_2C@C/Co@C.

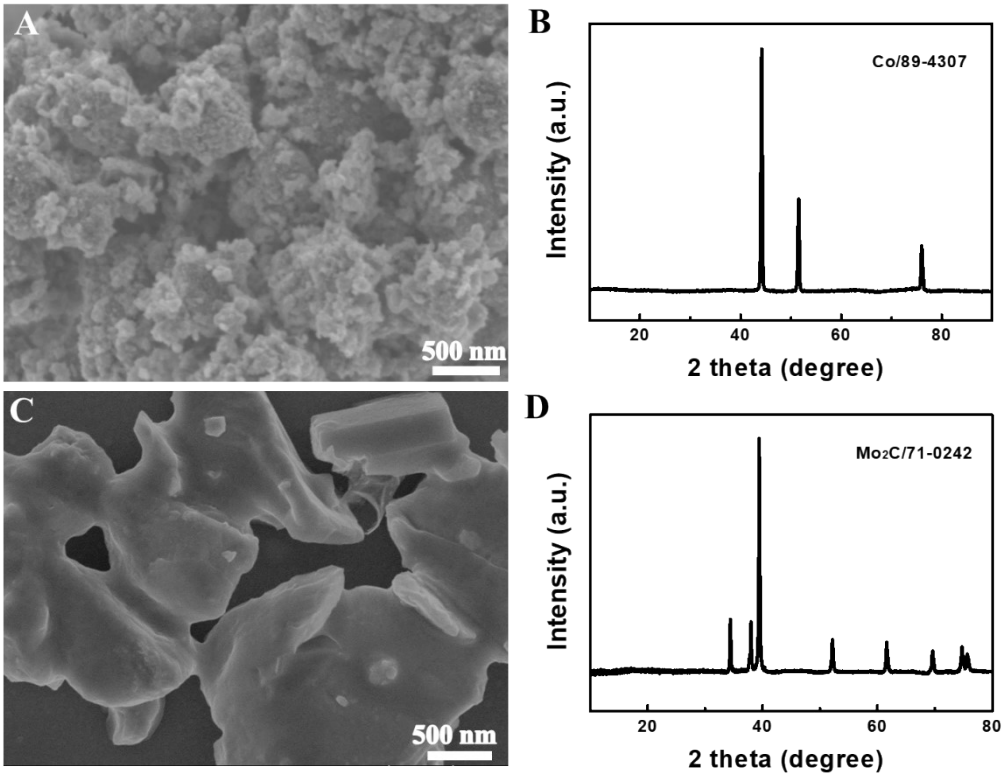

Figure S7. A), C) SEM image and B), D) XRD pattern of A-B) Co NPs and C-D) Mo_2C.

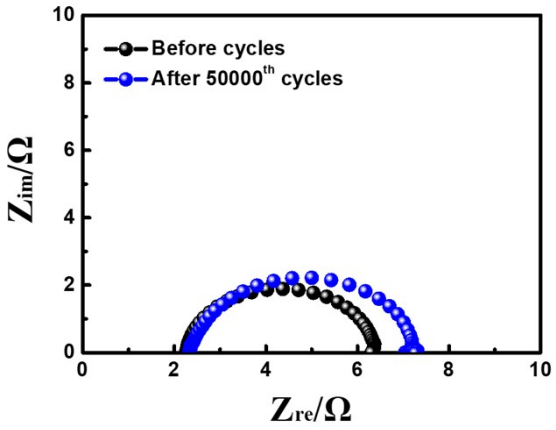

Figure S8. The EIS curves before and after 50000th CV sweeps of HER at 100 mV/s.

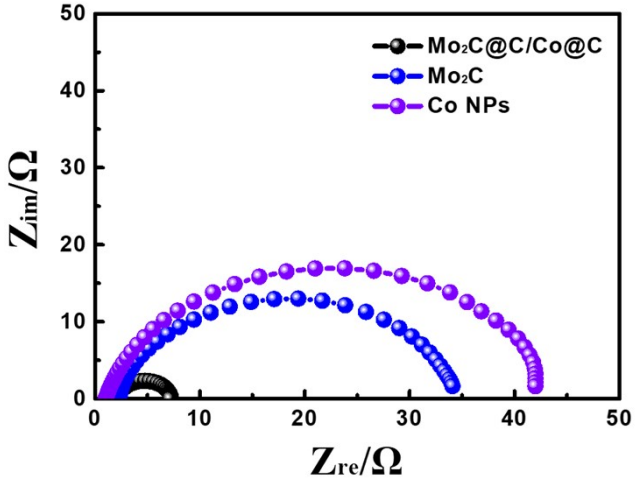

Figure S9. Nyquist plots of Mo_2C@C/Co@C, Mo_2C and Co NPs tested at the same overpotential of 300 mV.

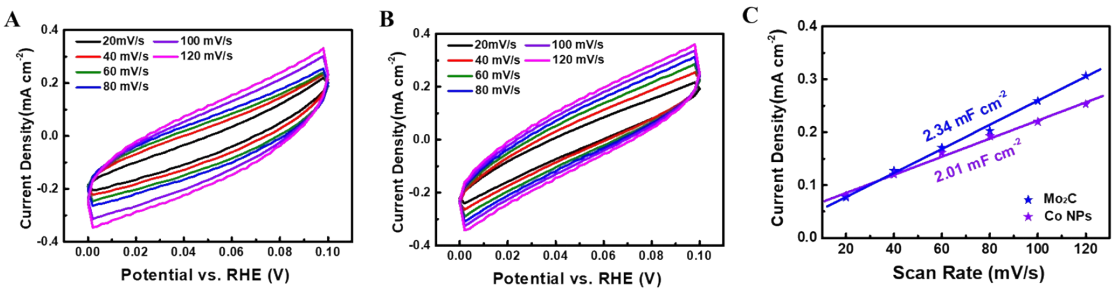

Figure S10. CV curves of (A) Mo_2C and B) Co NPs tested at various scan rates from 20 to 120 mV s^{-1} in the potential range of 0-0.1 V. (C) Scan rate dependence of the current densities of Mo_2C and Co NPs.

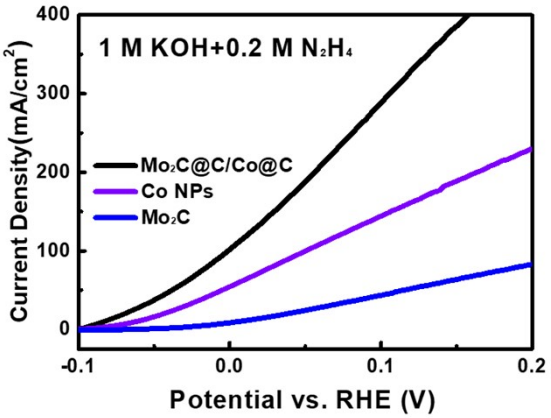

Figure S11. The comparing HzOR LSV curves tested in 1.0 M KOH with 0.2 M N_2H_4.

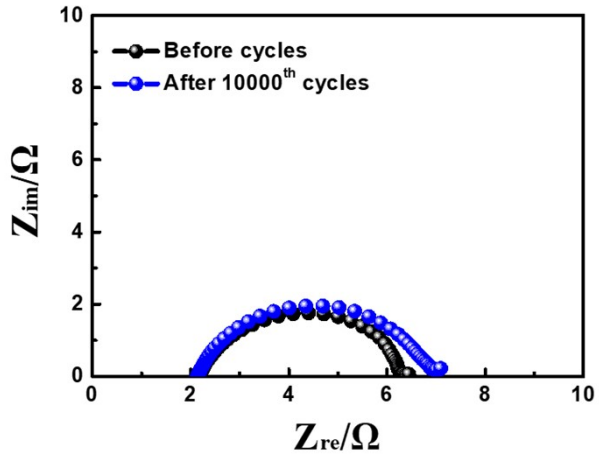

Figure S12. Nyquist plots of Mo_2C@C/Co@C tested before and after 10000 cycles for HzOR.

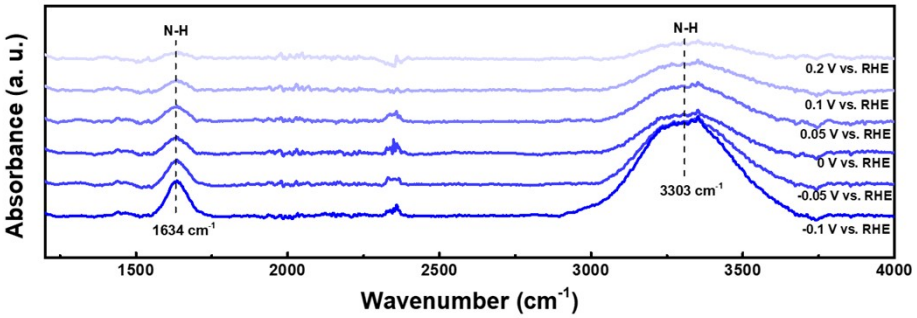

Figure S13. Potential-dependent in-situ FTIR spectra of Mo_2C@C/Co@C tested during the voltage of -0.1-0.2 V.

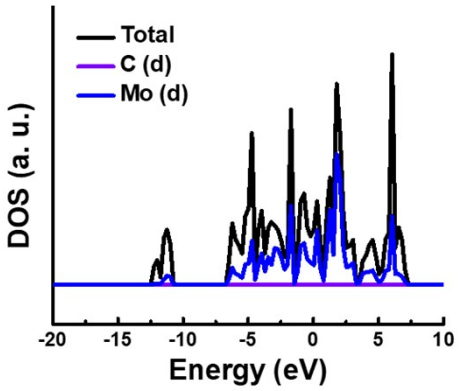

Figure S14. Total and partial density of states (DOS) calculated for Mo_2C.

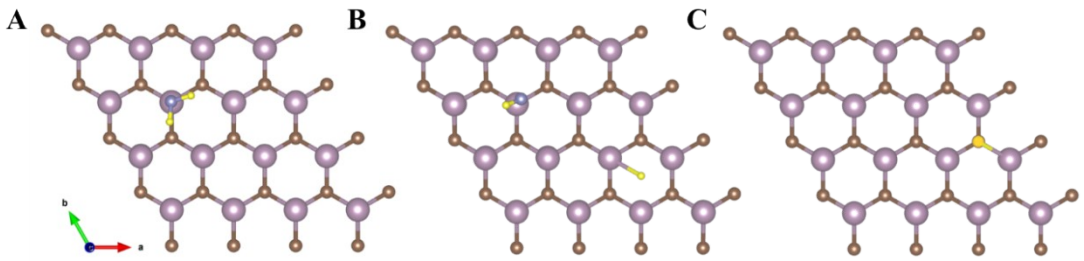

Figure S15. The water and hydrogen adsorption configurations of Mo_2C at different directions.

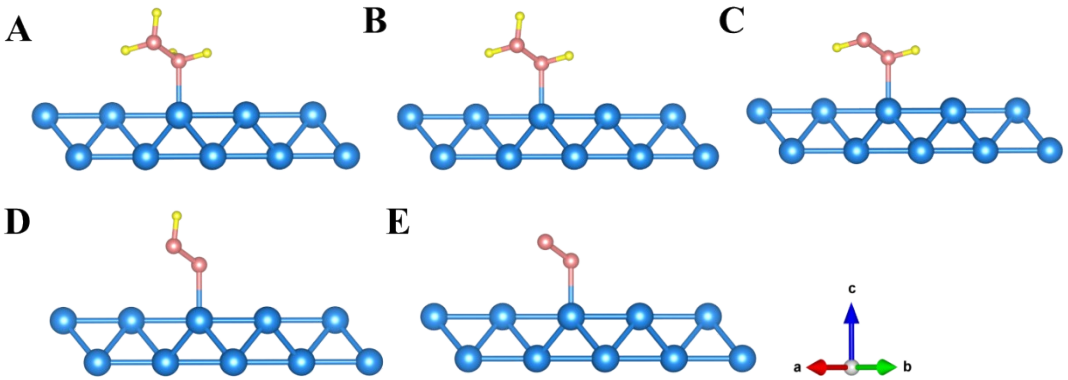

Figure S16. The atomic structure models of Co adsorbing N_2H_4 at different steps in different directions.

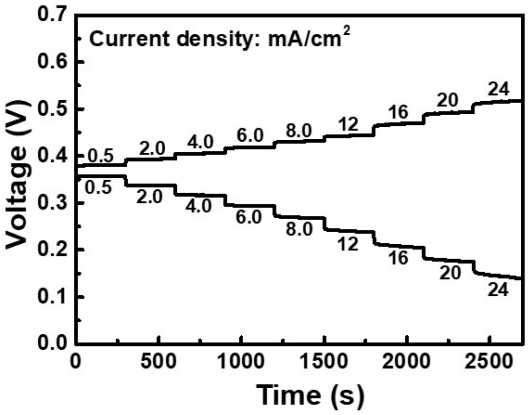

Figure S17. Galvanostatic discharge/charge curves at various current densities from 0.5 to 24 mA/cm^2.

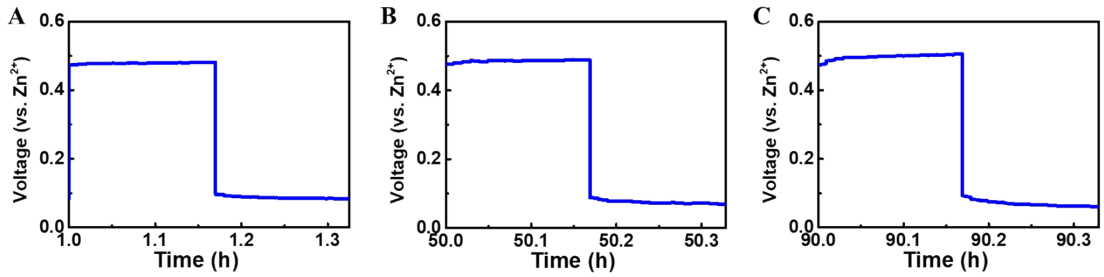

Figure S18. Partly enlarged galvanostatic discharge-charge cycling curves at 20 mA/cm^2.

Catalyst	η_{10} (mV vs. RHE)	Tafel slope (mV/dec)	Ref.
Mo_2C@C/Co@C	71	46.1	This work
Ni-Mo_2C-CNF	196	54.7	J. Colloid Interface Sci., 2020, 558, 100
β-Mo_2C Nanobelts	110	49.7	Appl. Catal. B-Environ., 2018, 224, 533
Ni-Mo_2C/NC@NF	40	54	Appl. Catal. B-Environ., 2021, 292, 120168
S-Mo_2C/CC	121	64.7	Appl. Catal. B-Environ., 2023, 322, 122131
MoO_2-Mo_2C-NC@CC-950 ◦C	79	59.7	Chem. Eng. J., 2023, 469, 143908
Co_2P/Mo_2C/Mo_3Co_3C@C	182	68	J. Mater. Chem. A, 2018, 6, 5789
Mo_2C/Mo_3N_2/C	76	52.6	J. Mater. Chem. A, 2023, 11, 6581
Mo_2C NWAs/CFP	170	72	Adv. Funct. Mater., 2018, 28, 1804600

Mo_2C/C	164	66	Small Methods, 2021, 5, 2100334
MoC-Mo_2C	114	62	Nat. Commun., 2021, 12, 6776
Mo_2C@NCS	132	78	Appl. Catal. B-Environ., 2020, 263, 118352
Ni/Mo_2C (1:2)-NCNFs	143	57.8	Adv. Energy Mater., 2019, 9, 1970027
Coral-like Mo_2C	110	73.9	Chem. Eng. J., 2023, 451, 138977.
Co/β-Mo_2C@N-CNTs	170	92	Angew. Chem. Int. Ed., 2019, 58, 4923
MoP-Mo_2C/NPC	120	50.3	Chem. Eng. J., 2022, 431,133719
H-Mo_2C/NG	63	48	Nat. Commun., 2022, 13, 7225
Co_2P/Mo_2C@NC	86	46	Appl. Catal. B-Environ., 2022, 310, 121354.

Table S1. Summary of some recently reported Mo_2C-based HER catalysts in alkaline electrolytes.

Catalyst	Electrolyte	η_{10} (mV vs. RHE)	Tafel slope (mV/dec)	Ref.
Mo_2C@C/Co@C	1.0 M KOH + 0.2 M N_2H_4	-83	13.6	This work
CoH-CoPV@CFP	1.0 M KOH + 0.4 M N_2H_4	-61	59.9	Appl. Catal. B-Environ., 2024, 345, 123661.
CC@CoNC-600	1.0 M KOH + 0.5 M N_2H_4	-61	49	Small, 2023, 19, 2300019
MoO_2/Co–NF	1.0 M KOH + 0.5 M N_2H_4	-73	22.9	J. Mater. Chem. A, 2022, 10, 17297
p-Co/CF	1.0 M KOH + 0.05 M N_2H_4	-150	8.83	Energy Environ. Sci., 2022, 15, 3246
Co_3Ta/C NP	3.0 M KOH + 0.2 M N_2H_4	-86（η_0）	56.9	Nat. Commun., 2019, 10, 4514
Ru-Co_3O_4	1.0 M KOH + 1.0 M N_2H_4	-24（η_{100}）	44	Adv. Funct. Mater., 2024, 34, 2311063
CoN-Co_2N@NF	1.0 M KOH + 0.1 M N_2H_4	-26（η_{100}）	42	Small, 2024, 20, 2306100
NiCoP/NF	1.0 M KOH	-83（η_{100}）	14	ACS Nano, 2023,

	+ 0.2 M N_2H_4			17, 10965
N-Ni_5P_4@CoP/CFP	1.0 M KOH	-32	24.9	Appl. Catal. B-
	+ 0.1 M N_2H_4			Environ., 2023,
				324, 122207.
PW-Co_3N NWA/NF	1.0 M KOH	-55	14	Nat. Commun.,
	+ 0.1 M N_2H_4			2020, 11, 1853

Table S2. Summary of some reported Co-based HzOR catalysts.